Chinese Chemical Letters 37 (2026) 111396

Contents lists available at ScienceDirect

Chinese Chemical Letters

journal homepage: www.elsevier.com/locate/cclet

Multi-scale delivery dynamics of tetrahedral framework nucleic acids: From organ accumulation to subcellular targeting and precision engineering strategies

Wen Chen[1], Hao Wang[1], Qiang Sun, Shaojingya Gao, Yunfeng Lin, Yun Wang*, Xiaoxiao Cai*

State Key Laboratory of Oral Diseases, National Center for Stomatology, National Clinical Research Center for Oral Diseases, West China Hospital of Stomatology, Sichuan University, Chengdu 610041, China

ARTICLE INFO

Article history:
Received 23 March 2025
Revised 25 May 2025
Accepted 28 May 2025
Available online 2 June 2025

Keywords:
Tetrahedral framework nucleic acids
Administration route
Biodistribution
Transmembrane transport mechanism
Subcellular localization

ABSTRACT

Tetrahedral framework nucleic acids (tFNAs), a novel class of nanodelivery carriers, demonstrate significant potential due to their well-defined topological structure, programmable molecular recognition capabilities, and exceptional biocompatibility. This article systematically reviews the dynamic behavior of tFNAs across multi-scale delivery processes. At the macroscale, it elucidates the organ accumulation and metabolism of tFNAs following various routes of administration. At the microscale, it delves into the transmembrane transport mechanisms and subcellular localization characteristics of tFNAs. Furthermore, this review discusses the current research status of strategies aimed at improving the delivery efficiency of tFNAs through active targeted modifications and proposes cutting-edge approaches to developing precision delivery systems leveraging engineering modifications and intelligent response designs.

© 2026 Published by Elsevier B.V. on behalf of Chinese Chemical Society and Institute of Materia Medica, Chinese Academy of Medical Sciences.

1. Introduction

Since Nadrian Seeman pioneered DNA nanotechnology in 1982, this interdisciplinary field has revolutionized nanoscale engineering by transforming DNA from a genetic information carrier into a programmable construction material [1,2]. DNA nanotechnology focuses on the use of DNA molecules for the precise design and manipulation of nanostructures, aiming to develop functional nanostructures for diverse applications, including drug delivery, diagnostic technology, and nanoelectronics [3–5]. The precise principles of Watson-Crick base pairing are leveraged to transform DNA nanostructures into meticulously designed complex architectures such as DNA origami and DNA tiles [6–9]. Through strategic sequence design and topological manipulation, researchers have developed an array of DNA-based architectures, including 2D lattice formations, polyhedral frameworks, and dynamic nanomachines capable of conformational changes in response to environmental stimuli. These programmable features, combined with the inherent biodegradability and low cytotoxicity of DNA, have positioned nucleic acid nanostructures as particularly promising candidates for biomedical applications [10–14].

Among these nanostructures, tetrahedral framework nucleic acids (tFNAs), first proposed by Turberfield, have garnered significant research attention [15]. Formed through the self-assembly of four complementary single-stranded DNAs, tFNAs exhibit a mechanically stable tetrahedral configuration, and their simple and efficient synthesis facilitates high yields of up to 90% [16]. This structural stability contributes to unique advantages over conventional DNA nanostructures, including low immunogenicity, rapid and efficient cellular uptake without the need for transfection reagents, and the ability to permeate biological tissues such as skin and mucous membranes [17,18]. Their structural rigidity enhances resistance to nuclease degradation while retaining a compact size that enables efficient biological interactions. tFNAs can also be engineered for site-specific drug loading through mechanisms such as covalent bonding, sticky-end ligation, or other alternative connection strategies [19–21]. For example, oligonucleotides or anti-oligonucleotides can be attached to the middle or end of single-stranded DNAs [22–24]; small-molecule drugs can be incorporated into double-stranded DNAs *via* electrostatic adsorption [25–30]; chemical cross-linking can be achieved between two single-stranded DNAs (ssDNA) through base complementary pairing [31–33]. Additionally, functional modifications can equip tFNAs

* Corresponding authors.
E-mail addresses: wy630ivy@outlook.com (Y. Wang), xcai@scu.edu.cn (X. Cai).
[1] These authors contributed equally to this work.

https://doi.org/10.1016/j.cclet.2025.111396
1001-8417/© 2026 Published by Elsevier B.V. on behalf of Chinese Chemical Society and Institute of Materia Medica, Chinese Academy of Medical Sciences.

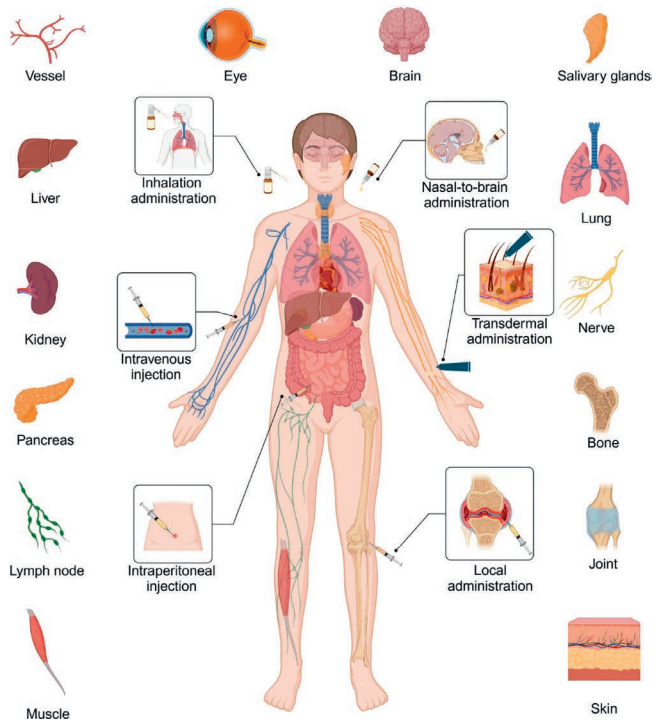


Fig. 1. Administration routes, distribution organs and tissues of tFNAs. Created in BioRender.

with the ability to target precise cellular locations and respond to specific stimuli for controlled drug release [34,35]. Owing to these unique properties, tFNAs have become a focal point of research in the biomedical field, with applications spanning bioimaging, biosensing, molecular diagnostics, gene delivery, disease treatment, and regenerative medicine.

The use of nanomaterials for drug delivery involves a multilevel progression, from systemic-level organ distribution to subcellular compartmentalization, highlighting the need to investigate the *in vivo* biodistribution patterns and transmembrane transport mechanisms. Systematic research in these areas and special designs help optimize therapeutic efficacy while reducing off-target effects. After years of development, tFNAs have become a robust delivery system for addressing key medical and health challenges. This review concentrates on recent advancements in the administration routes, biodistribution, and organ-targeting ability of tFNAs (Fig. 1). Additionally, the transmembrane transport mechanisms, subcellular localization, and the subcellular design strategies and applications of tFNAs are explored.

2. Structural design, synthesis, and characteristics of tFNAs

tFNAs are self-assembled nanostructures formed by four specifically designed ssDNA. These strands contain complementary regions that enable precise three-dimensional tetrahedral assembly through Watson-Crick base pairing. The resulting structure features six double-stranded DNA edges and four vertices, each stabilized by three unpaired nucleotides. This configuration ensures structural integrity while retaining localized flexibility [36]. The size and functional properties of tFNAs can be precisely modulated by adjusting the length or sequence of ssDNA components, demonstrating the inherent programmability of nucleic acid-based nanostructures.

The synthesis of tFNAs primarily relies on a one-step thermal annealing process. Among available assembly strategies, including single-strand annealing, three-way junction assembly [37], and DNA origami [38], the single-strand annealing method is predominantly adopted due to its simplicity and high yield. In a typical procedure, equimolar concentrations of four ssDNA strands are mixed in Tris–HCl buffer containing $MgCl_2$. The solution is heated to 95 °C for 10 min to denature secondary structures, followed by rapid cooling to 4 °C for 20 min to facilitate controlled hybridization and structural formation [39].

As nucleic acid-based nanoparticles, tFNAs exhibit a particle size of tens of nanometers and a negative surface charge. Studies have shown that tFNAs exhibit high compressive strength and maintain stability under various loads, which reflects the excellent mechanical properties given to them by the tetrahedral geometry [40]. This structural robustness, combined with steric hindrance at vertices and edges, enhances resistance to enzymatic degradation in physiological environments, prolonging their *in vivo* retention time [41]. As nanoparticles, tFNAs achieve transfection reagent-free cellular uptake *via* endocytosis while maintaining structural integrity intracellularly [42].

Functionally, tFNAs demonstrate intrinsic anti-inflammatory and antioxidant activities, enabling modulation of diverse cellular phenotypes such as proliferation, migration, apoptosis, pyroptosis, differentiation, and autophagy [43]. Their programmable vertices and edges further allow site-specific conjugation of therapeutic cargoes (*e.g.*, RNA, proteins, or small-molecule drugs). These combined attributes establish tFNAs as versatile platforms for biomedical applications ranging.

3. Biodistribution of tFNAs

The size, shape, surface charge, material composition, and administration route of nanomaterials collectively determine their localization within specific organs [44–46]. A thorough understanding of nanomaterials' biodistribution is crucial for optimizing their effectiveness as delivery vectors. The administration route, in particular, is a key factor, and different routes function in different ways. For example, intravenous injection (IV) enables rapid systemic circulation but risks accelerated clearance, whereas transdermal delivery must overcome the skin barrier for effective permeation. These routes influence not only the initial biodistribution of nanomaterials but also their dynamic accumulation and metabolic patterns at the organ, tissue, and cellular levels. Understanding route-dependent biological mechanisms is essential for enhancing the nanocarrier's targeting precision, minimizing off-target effects, and optimizing therapeutic outcomes. tFNAs, a novel class of nanoparticles, exhibit unique structural and physicochemical properties. They are self-assembled from four single-stranded DNAs through base complementary pairing, and each nanoparticle possesses a diameter of approximately 10 nm, a zeta potential of around −9 mV, and a tetrahedral morphology [39]. Despite their potential, systematic analyses of the *in vivo* distribution of tFNAs remain limited. To bridge this gap, we reviewed and synthesized data from current applications. tFNAs are primarily administered to various disease models *via* intravenous, intraperitoneal, and local injections, as well as transdermal, inhalation, and nasal-to-brain routes. Their predominant accumulation sites include the liver, kidney, pancreas, and lymph nodes. To further enhance tFNAs' targeting ability and delivery efficiency, aptamer modifications can be employed to enhance accumulation in specific organs and cells.

3.1. Administration routes

tFNAs can be administered through multiple routes to accommodate the needs of various diseases. IV, with its direct entry into the bloodstream, enables rapid systemic distribution of the drug. After IV, tFNAs quickly distribute throughout the body and are primarily metabolized by the liver and kidneys (Fig. S1 in Supporting

information) [47]. Intraperitoneal injection is another systemic administration route that can serve as an alternative to IV (Fig. S2 in Supporting information) [48]. Local injection significantly increases local drug concentration in specific anatomical regions, with retention time varying depending on the injection site (Fig. S3 in Supporting information) [49,50]. Transdermal administration leverages the tissue penetration properties of tFNAs to achieve non-invasive treatment, effectively treating skin diseases (Fig. S4 in Supporting information) [51]. tFNAs can also be administered *via* inhalation to achieve significant accumulation in the lungs, thereby treating pulmonary inflammation (Fig. S5 in Supporting information) [52]. The nasal-to-brain administration allows tFNAs entry into the brain through the nasal mucosa-neural pathway, offering a high-efficiency, low-toxicity approach for central nervous system diseases (Fig. S6 in Supporting information) [53]. Detailed information on multi-administration routes of tFNAs is provided in Supporting information.

3.2. Distribution organs and tissues

Following administration *via* specific delivery routes, tFNAs exhibit preferential accumulation in target organs and tissues. Their biodistribution varies remarkably due to differences in anatomical architecture and histological composition. This section outlines the structural characteristics of major organs and tissues and provides a comprehensive analysis of tFNA distribution within these compartments, followed by a summary of tFNAs' biomedical applications in diseases involving these areas.

3.2.1. Liver

The liver serves as the main target of nanomaterials after entering systemic circulation, and significant liver accumulation occurs following both intramuscular and IV. Consequently, hepatotoxicity assessment is pivotal for examining the *in vivo* application of nanomaterials [54]. Numerous metal-based nanomaterials induce hepatic steatosis or oxidative stress, which limits their clinical utility [55,56]. Upon entering the liver, nanomaterials undergo clearance through a multi-tiered biological mechanism [57,58]. This process is mainly related to the physical filtration of liver structure, the clearance of Kupffer cells, sinusoidal endothelial cells and hepatic stellate cells [59,60]. Due to the passive liver-targeting properties, tFNAs present a viable therapeutic strategy for liver disease treatment. Chen *et al*. established an acute liver injury model and demonstrated that tail vein-injected tFNAs accumulated rapidly in the liver within 30 min post-administration [61], effectively alleviating liver damage and promoting liver regeneration by regulating the cell cycle and P53 signaling pathway. In a study by Zhang *et al*. [62], tFNAs and mesenchymal stem cells were injected into mice through the tail vein and accumulated in the liver after 30 min. tFNAs facilitated the homing of mesenchymal stem cells to the liver and hepatogenic differentiation, thereby promoting liver repair.

3.2.2. Kidney

The kidneys excrete nanomaterials in urine, which is the most efficient route for nanomaterial metabolism in the body. During this process, the nanomaterials are directly excreted from the body, exhibiting minimal interaction with tissues, thereby reducing potential toxic side effects from nanomaterial decomposition [63]. However, due to size (6–8 nm) and charge (neutral) constraints imposed by the basement membrane pore size and charge-selective barrier, many nanomaterials cannot be cleared *via* this pathway. When nanomaterials evade glomerular filtration and deposit in the kidneys, they can cause severe damage after nanomaterial exposure, particularly targeting glomerular mesangial cells, glomerular capillary beds, and proximal tubular epithelial cells [64,65]. As a result, nephrotoxicity is a critical indicator for the biocompatibility of nanomaterials. The particle size of tetrahedral tFNAs approximates the renal excretion threshold, potentially enabling passive kidney targeting. In a murine model of acute kidney injury established by Zhang *et al*. [66], pronounced fluorescent signals were detected in the kidneys within 30 min after intravenous tFNA administration. These nanoparticles mitigated oxidative stress and cellular apoptosis, thereby contributing to injury treatment. Building upon this, Yan *et al*. conjugated coumarin glycosides to tFNAs, strengthening the therapeutic efficacy against acute kidney injury through mitochondrial protection [27]. The experimental results revealed that nanomaterials in the kidneys peaked at 2 h after IV and mainly accumulated in renal tubules. Notably, damaged kidneys exhibited greater tFNAs uptake than healthy ones.

3.2.3. Brain

As the central organ of the nervous system, the brain plays a pivotal role in maintaining organismal homeostasis. Neurodegenerative and neuroinflammatory disorders, including Alzheimer's disease, Parkinson's disease, stroke, and multiple sclerosis, exhibit multifactorial pathogenesis and often lead to severe neurological deficits [67]. The blood-brain barrier (BBB), an evolutionarily conserved structure that safeguards brain homeostasis, simultaneously impedes therapeutic drug delivery [68]. Local intracranial injection, although direct, is highly invasive and carries a high risk of tissue damage. Intravenous administration, a conventional approach for brain-targeted delivery, suffers from limited brain accumulation due to BBB exclusion. In contrast, tFNAs efficiently traverse the BBB and achieve brain enrichment due to their suitable nanoscale dimensions and good structural integrity, and these capabilities position them as promising nanocarriers [69–71]. Additionally, as they can enhance cellular proliferation, attenuate oxidative stress, and offer a high capacity for functionalization, these nanoparticles demonstrate therapeutic potential in managing epilepsy [72], depression [69], and multiple sclerosis [73]. Nasal-to-brain delivery, a non-invasive strategy bypassing the BBB, offers advantages over systemic delivery but requires robust nasal mucosal penetration and resistance to mucociliary clearance. Zhang *et al*. examined the feasibility of intranasal tFNA delivery and showed their transport *via* olfactory/trigeminal pathways and broad distribution across multiple brain regions [53]. Similarly, Tan *et al*. reported that nasally administered tFNAs inhibited Aβ-induced ferroptosis and ameliorated cognitive/synaptic dysfunction in Alzheimer's disease models [74], further validating this approach.

3.2.4. Lung

The lungs, directly exposed to the external environment, readily encounter airborne nanoparticles. The deposition site of nanomaterials is closely related to particle size. Larger particles preferentially settle in the trachea and bronchi lined with ciliated epithelial cells, whereas smaller particles are more likely to reach the peripheral alveolar regions of the lungs [75,76]. Once in the alveolar area, nanomaterials can be endocytosed by macrophages and degraded within lysosomes. Unphagocytosed small particles may traverse the tight junctions between alveolar epithelial cells, entering the pulmonary interstitium. Due to the extensive vascularization of the lungs, intravenous administration remains a viable strategy for managing pulmonary diseases. In a murine model of sepsis, Chen *et al*. demonstrated that intravenous administration of tFNAs effectively alleviated pulmonary inflammation [77]. Inhalation therapy, characterized by non-invasiveness, low systemic exposure, and site-specific delivery, represents an advantageous approach for pulmonary drug delivery. Yao *et al*. developed an inhalable DNA tetrahedral miRNA sponge, which exhibited post-inhalation cellular uptake rates of 22.53 % ± 2.58 % in lung epithelial cells, 15.83 % ± 0.66 % in macrophages, and 15.85 % ± 2.45 % in neutrophils [52].

This formulation significantly mitigated LPS-induced acute lung injury by targeting key inflammatory pathways.

3.2.5. Pancreas

The pancreas is a gland with both endocrine and exocrine functions. The exocrine function mainly involves the secretion of various digestive enzymes into the intestinal lumen to aid chyme transport and further digestion, while the endocrine function regulates blood sugar levels through insulin and glucagon secretion, thereby playing a vital role in maintaining systemic glucose homeostasis [78,79]. Delivering therapeutics to the pancreas presents significant challenges as the blood-pancreatic barrier and its complex microenvironment can influence drug release and bioactivity [80]. tFNAs possess the capability to overcome these challenges and treat pancreatic disorders. In a study by Wang *et al.* [81], tFNAs accumulated significantly in the pancreata of mice with taurocholic acid-induced severe acute pancreatitis following tail vein administration, effectively reducing inflammatory responses and protecting pancreatic cells. Additionally, liver, kidney, and lung damage associated with severe acute pancreatitis was alleviated. In the diabetic model developed by Gao *et al.* [82], tFNAs reached the pancreas *via* tail vein injection and treated type 1 diabetes by restoring the pancreatic immune microenvironment and protecting β cells.

3.2.6. Salivary glands

The salivary glands comprise a diverse population of acinar cells, ductal cells, myoepithelial cells, and immune cells, all essential for saliva production and secretion, processes crucial for oral and systemic health [83]. Xie *et al.* addressed radiation-induced salivary gland damage by intravenously administering tFNAs [84]. They observed a substantial nanomaterial accumulation in damaged glands 45 min post-administration, with minimal retention after 90 min. Additionally, damaged salivary glands exhibited significantly higher tFNA concentrations than healthy ones. In another study [85], Gao *et al.* found that intravenously administered tFNAs effectively reduced excessive T and B cell activity within the salivary glands, ameliorating Sjögren's syndrome and enhancing the tissue architecture and functional integrity of the radiation-damaged glands.

3.2.7. Lymph nodes

Lymph nodes, a critical component of the systemic immune system, contain large numbers of lymphocytes, macrophages, and antigen-presenting cells. Peripheral antigens are phagocytosed and presented to lymph nodes, where they activate T and B cells and regulate adaptive immune responses to foreign antigens [86]. Research has confirmed that the intensity of vaccine-activated immune responses is related to the transport efficiency of antigen-presenting cells to lymph nodes [87]. Leveraging lymph nodes to activate systemic immune responses is a promising therapeutic strategy, though challenges remain in vaccine delivery. Shen *et al.* found that subcutaneously injected tFNAs accumulated significantly in lymph nodes while maintaining a certain degree of integrity [88]. A coronavirus disease 2019 (COVID-19) peptide vaccine developed using this approach induced memory B and T cells in mice and enhanced *in vivo* antibody titers. Qin *et al.* conjugated miRNA-155, a regulator of immune function, to tFNAs and administered the complex intraperitoneally [89]. High concentrations of the nanomaterial were detected in lymph nodes within 5 min, followed by a gradual decline within 20 min. Notably, T-155 preferentially accumulated in the lymph nodes of mice before reaching the liver and kidneys, highlighting its ability to efficiently and rapidly target lymph nodes for immune modulation.

3.2.8. Skin

The skin, the largest and most accessible organ in humans, serves as a promising platform for non-invasive drug delivery due to its unique anatomical structure. Beyond traditional systemic injections [90], transdermal delivery of nanomaterials functions *via* three primary pathways: (1) Intercellular route (diffusion through lipid-rich extracellular spaces), (2) transcellular route (direct penetration through keratinocytes and lipid bilayers), and (3) appendageal route (*via* hair follicles, sweat glands, or sebaceous glands). Intercellular transport efficiency is predominantly governed by nanoparticle size and flexibility, while the transcellular pathway requires nanomaterials to exhibit a hydrophilic-lipophilic balance for traversing alternating hydrophilic and lipophilic cellular domains. Although the appendageal pathway enables rapid deep-skin penetration, its efficacy depends heavily on hair follicle density and distribution [91]. A study by Christian *et al.* [92] demonstrated that framework nucleic acids preferentially accumulated in hair follicles and sebaceous glands, with 20 %–25 % of administered nanoparticles entering the skin *via* non-appendageal routes. Notably, tFNAs exhibited superior transdermal penetration capacity, reaching the dermal layer while maintaining structural integrity. These findings underscore the therapeutic potential of tFNA-based transdermal systems in addressing wound healing [93,94], anti-aging [33], photodamage [95], and psoriasis [51].

3.2.9. Eye

The eye facilitates the conversion of light signals into neural electrical signals through its optical system, neural circuitry, and metabolic regulatory mechanisms. Anatomically, the eye is divided into the anterior segment (from the cornea to the posterior lens capsule) and the posterior segment (from the posterior lens capsule to the retina) [96,97]. For ocular surface and anterior segment diseases, topical administration *via* eye drops is the primary therapeutic approach [98]. However, conventional drugs are often limited by rapid tear clearance, with minimal drug penetration into intraocular tissues [99]. tFNAs demonstrate enhanced corneal permeability. Liu *et al.* employed a rabbit model of corneal alkali burn and observed that topical tFNA application significantly accelerated corneal epithelial healing [100]. In contrast, posterior segment diseases are poorly responsive to topical therapies, while systemic drug delivery fails to achieve therapeutic concentrations due to the blood-aqueous barrier and blood-retinal barrier [101]. To address these challenges, periocular and intravitreal injection routes are applied for posterior segment drug delivery. Wang *et al.* investigated the intraocular distribution of tFNAs following subconjunctival injection [102] and observed retinal penetration of tFNAs, with fluorescent signals persisting for up to 24 h, highlighting the potential of periocularly administered tFNAs in treating posterior segment pathologies.

3.2.10. Bone

Bone defects, commonly arising from conditions such as infections, genetic disorders, trauma, and tumors, can lead to clinically significant deformities and functional impairments. Bone regeneration is a highly orchestrated process involving coordinated cell proliferation, differentiation, migration, and extracellular matrix deposition [103–106]. Applications of tFNAs for bone regeneration have been extensively studied. Liu *et al.* demonstrated that systemic tFNA administration enhanced vascular network formation, callus formation, and osteogenesis in aged osteoporotic fracture models [107]. Although stem cell therapy represents a promising approach for bone defect repair, its clinical translation is limited by low survival rates and differentiation efficiency at lesion sites. Previous studies show that tFNAs significantly enhance the proliferation, migration, and osteogenic differentiation of multiple stem cell types, including bone marrow mesenchymal stem cells [108], adipose-derived stem cells [109], and dental follicle stem cells [110]. This pro-regenerative modulation of stem cell behavior may underlie the osteogenic potential of tFNAs [111].

3.2.11. Muscle

Muscle tissue, comprising bundles of multinucleated muscle fibers, accounts for approximately one-third of adult body weight. Muscle damage or degeneration exerts profound effects on body morphology and function. Satellite cells, a population of adult stem cells essential for muscle regeneration, decline in quantity and activity with aging, impairing muscle regeneration capacity [112]. Notably, tFNAs exhibit a marked ability to promote proliferation and migration across diverse cell types, including satellite cells. Gao *et al*. administered tFNAs locally at injury sites in mice with acute muscle damage [113]. Their findings demonstrated that tFNAs increased myoblast recruitment and accelerated muscle tissue repair. Yu *et al*. applied tFNAs to a sarcopenia model and found that tFNAs attenuated muscle atrophy and improved muscle strength *via* mitochondrial protection [114].

3.2.12. Joint

Joints comprise articular capsules, bones, cartilages, synoviums, and ligaments. Pathological conditions such as autoimmunity, infection, or trauma trigger joint inflammation, leading to structural degradation, cartilage erosion, and synovial hyperplasia [115,116]. Targeted nanoparticle delivery to joints represents a promising therapeutic strategy. Nanoparticle biodistribution in joints is strongly influenced by particle size: those smaller than 300 nm can readily diffuse into systemic circulation from the joint capsule, whereas larger nanoparticles exhibit limited joint penetration following systemic administration [117]. Liao *et al*. observed sustained retention (over 180 min) of intra-articularly injected tFNAs in the temporomandibular joint [118]. Zhang *et al*. explored how intravenously administered tFNAs accumulated in the joints of rheumatoid arthritis mice and observed selective accumulation in inflamed tissues, not in healthy joints, as evidenced by fluorescent signals [35]. This highlights the preferential uptake of tFNAs by pathologically altered tissues. Additionally, tFNAs enhance cellular proliferation and migration in the joint microenvironment. Fu *et al*. reported that intra-articular delivery of tFNAs promoted articular cartilage repair by synovial mesenchymal stem cells through transforming growth factor beta (TGF-β)/small mother against decapentaplegic 2/3 (Smad2/3) signaling pathway modulation [119].

3.2.13. Blood vessels

Blood vessels form a closed tubular network throughout the human body, responsible for oxygen and nutrient delivery and metabolic waste removal [120–122]. Angiogenesis is critical for tissue regeneration. Lin *et al*. administered tFNAs around mucosal ulcers in diabetic rats [123]. Histological analysis revealed a significant enhancement in wound vascularization, epithelialization, collagen deposition, and tissue organization, which accelerates wound healing. Ge *et al*. further improved angiogenic capacity by loading miRNA-126 onto tFNAs, which were subsequently internalized by vascular endothelial cells [124]. Suppressing pathological angiogenesis represents an effective strategy for anti-tumor therapy. Although tFNAs promote physiological angiogenesis, their drug payloads can be modulated to inhibit abnormal blood vessel formation. Tang *et al*. used tFNAs to deliver anti-Fms-like tyrosine kinase-1 (anti-Flt1) peptides *via* IV to mice with triple-negative breast cancer [125]. These nanoparticles accumulated preferentially in tumor tissues and targeted vascular endothelial growth factor receptor 1 (VEGFR1), effectively suppressing tumor-associated pathological angiogenesis and tumor progression.

3.2.14. Nerve

Nerves, composed of neurons and glial cells, form critical pathways for transmitting sensory and motor signals throughout the body [126]. This section focuses on peripheral nerves. tFNAs are predominantly delivered *via* local injection to exert neuroprotective and regenerative effects. Yao *et al*. administered tFNAs *via* perineural injection in a rat model of facial nerve crush injury [127]. Their findings revealed that tFNAs enhanced facial nerve regeneration by activating the nerve growth factor (NGF)/phosphatidylinositol 3-kinase (PI3K)/protein kinase B (AKT) signaling pathway. Notably, the therapeutic efficacy can be augmented through structural functionalization. Building on this, Li *et al*. loaded miRNA-22 onto tFNAs, which promoted Schwann cell-mediated macrophage recruitment and macrophage polarization toward the pro-regenerative M2 phenotype, thereby accelerating nerve repair [128].

3.3. Active targeting strategies

tFNAs exhibit significant potential in disease treatment due to their programmable structure and multiple administration routes. While systemic administration facilitates widespread drug distribution, likely leading to passive accumulation in the liver and kidneys, and local administration enables temporary retention at the target site, clinical applications still face limitations such as inadequate targeting precision and short retention times. To address these challenges, researchers have enhanced the targeted delivery capabilities of engineered tFNAs with chemical modifications to enhance their targeted delivery capabilities and thereby broaden their medical applications. Common strategies include target molecule guidance, smart responsive design, and biological barrier penetration. Wang *et al*. modified tFNAs with a transferrin receptor aptamer and loaded them with small activating RNAs (saRNAs) for pancreatic cancer treatment [129]. Two hours after tail vein injection, a significant nanodrug accumulation was observed at the tumor site, highlighting the enhanced active targeting ability of aptamer-modified tFNAs. In another study, the AS1411 aptamer, a DNA aptamer specific for nucleolin overexpressed in many tumor cells [130–133], enabled tFNAs to specifically recognize and bind to tumor cells, promoting rapid tumor accumulation [134]. Other modifications such as folic acid [135,136], tumor-penetrating peptides [137], and affimers [138] have demonstrated comparable tumor-targeting effects. To further refine tFNAs, Ma *et al*. incorporated drugs, aptamers, erythrocyte membranes, and pH-responsive functionalized liposomes for biomimetic camouflage [139]. This complex modification protects the drug from rapid clearance, extends its half-life, and enhances drug release in the tumor microenvironment, improving anti-tumor efficacy. Although tFNAs are primarily metabolized in the liver and kidneys, the incorporation of aptamers significantly increases drug concentration and retention time at the target site. Beyond tumor-targeting applications, modifications such as the 19-mer peptide derived from the Kunitz domain of human aprotinin enable tFNAs to penetrate the BBB [140], and thrombin aptamers hold promise for targeted thrombin ablation. DNA nanotechnology facilitates precise nanoparticle assembly within a size range suitable for targeted delivery to most organs, including the brain, lungs, liver, and lymph nodes. Other chemical modifications, such as thiol modifications studied by Shi *et al*. [141] and Lin *et al*. [142], have been shown to alter the surface properties of DNA nanostructures, enabling covalent bonding with lipid molecules to modulate hydrophilicity. Due to the exceptional programmability of tFNAs, engineering modifications help these nanoparticles meet diverse organ-targeting requirements.

The above content reviews the biodistribution of tFNAs. It is worth noting that the nucleic acid sequence composition may also affect the biological characteristics of tFNAs. Studies have shown that CpG motifs in nucleic acid chains can activate Toll-like receptor 9 (TLR9)-mediated immune responses and accelerate systemic clearance [143]. Most of the tFNAs used in current studies have the same sequence [88,144,145] and have been shown to have good biocompatibility [146], but there is a lack of systematic comparison of sequence-variant tFNAs. This gap has hindered the

elucidation of structure-activity relationships, especially in terms of how sequence-dependent molecular recognition mechanisms affect biodistribution patterns. Related research needs further exploration.

In summary, the unique physical properties of tFNAs make them suitable for various administration routes. Their structural rigidity and chemical stability allow them to maintain integrity and undergo gradual *in vivo* unwinding, a feature potentially relevant to programmed drug release. Depending on the administration route, tFNAs are primarily metabolized in the liver and kidneys, with no observed biological toxicity to vital organs, and these properties position these nanoparticles as promising nanodrug delivery platforms. However, further investigation into the mechanisms under their drug delivery routes, such as axonal transport and transdermal penetration, is necessary. A deep understanding of their biodistribution characteristics and the development of more effective delivery routes and strategies will enable precise nanoparticle localization in specific organs or tissues, thereby enhancing therapeutic efficacy.

4. Cellular transport mechanism of tFNAs

Following accumulation in the target area, tFNAs must be internalized by cells and, in some cases, transported to specific subcellular compartments. tFNAs demonstrate efficient cellular internalization, and preliminary studies have explored their uptake mechanisms in various cell types. Research suggests that upon cellular entry, tFNAs are often confined to the endosomal-lysosomal system, with some co-localization observed with organelles such as mitochondria. A systematic analysis of their localization patterns, including organelle-specific enrichment tendencies, can inform the development of carriers designed to enhance lysosomal escape, thereby increasing the effective concentration of drugs at the target site. Elucidating the cellular transport mechanisms of tFNAs is a critical scientific challenge in optimizing their function as intelligent drug carriers. This section reviews the prevalent cellular uptake pathways used by nanomaterials and summarizes current findings regarding the transmembrane transport mechanisms and subcellular localization characteristics of tFNAs. Furthermore, based on these insights, it proposes new applications for tFNAs in targeted subcellular structure intervention. A comprehensive understanding of the interactions between tFNAs and subcellular structures will establish a theoretical framework for precision delivery technologies and facilitate their application in more complex scenarios.

4.1. Common transmembrane transport mechanisms of nanomaterials

The cell membrane selectively regulates nanoparticle internalization primarily through endocytosis, which is broadly classified into phagocytosis and pinocytosis. Phagocytosis, executed by specialized immune cells, engulfs large particles (>250 nm) *via* membrane deformation and lysosomal degradation. Pinocytosis, ubiquitous across cell types, includes macropinocytosis (non-selective uptake of extracellular fluid) [147], clathrin-mediated endocytosis (CME, receptor-specific or nonspecific vesicular transport) [148,149], and caveolin-mediated endocytosis (CvME, cholesterol-rich vesicle formation evading lysosomal degradation) [150,151]. CME facilitates rapid internalization *via* ligand-receptor interactions, while CvME enables targeted delivery to non-degradative compartments. Additionally, clathrin/caveolin-independent pathways involving lipid rafts remain poorly understood [152]. Nanoparticle size, surface properties, and cell-specific factors dictate pathway preference, with engineered modifications (*e.g.*, aptamers or ligands) enhancing delivery efficiency by steering specific endocytic routes. Detailed mechanisms are provided in Supporting Information.

4.2. Transmembrane transport mechanism of tFNAs

Due to the polyanionic nature of DNA, there is typically significant electrostatic repulsion between DNA and negatively charged cell membranes, which hinders the efficient uptake of unmodified DNA oligonucleotides without transfection agents. However, pioneering research by Turberfield *et al.* [42] in 2011 demonstrated that tFNAs can be efficiently internalized by human embryonic kidney cells without transfection agents and retain their structural integrity for at least 48 h. Studies on how the shape and size of DNA nanostructures influence cellular internalization efficiency revealed that tetrahedral structures are more readily absorbed by cells in both 2D and 3D models compared to other geometric shapes [153]. Fan's group further elucidated the mechanism of tFNA entry into cells, showing that they are rapidly internalized into HeLa cells *via* caveolin-mediated endocytosis [154]. Subsequent analyses indicated that tFNAs approach the HeLa cell membrane at their vertices to minimize electrostatic repulsion, induce charge redistribution on the membrane under the influence of caveolin, and form caveolae vesicles to facilitate cellular entry (Fig. S7A in Supporting information) [155]. Subsequent screening using drug affinity responsive target stability (DARTS) and liquid chromatography/tandem mass spectrometry (LC-MS/MS) identified caveolin-1 (CAV1) and macropinocytosis-related sorting nexin 5 (SNX5) as key proteins interacting with tFNAs during endocytosis. Knockout experiments of CAV1 and SNX5 confirmed that both caveolin-mediated endocytosis and macropinocytosis mediate tFNAs' cellular uptake (Fig. S7B in Supporting information) [156]. Lin's team [31,33,157,158] employed small molecule inhibitors of various endocytic pathways across multiple cell types, including HeLa cells, mouse bone marrow stromal cells, human umbilical vein endothelial cells, and human keratinocytes, to further clarify that tFNAs intracellular entry is energy-dependent, caveolin-mediated, and requires the involvement of microfilaments, microtubules, and cholesterol. Additionally, the clathrin-mediated endocytic pathway and macropinocytosis contribute to tFNAs' cellular uptake to some extent (Fig. S7C in Supporting information). Researchers have also observed that the internalization mechanism of tFNAs varies by cell type, suggesting the potential existence of passive targeting mechanisms for specific cell types. Further studies have shown that framework nucleic acids with higher guanine content exhibit greater cellular uptake compared to those primarily composed of adenine, thymine, and cytosine [159], indicating that regulating sequence composition is a feasible strategy to enhance delivery efficiency.

4.3. Subcellular localization characteristics

The endocytic pathways of nanomaterials are closely linked to their intracellular transport processes. Vesicles formed through phagocytosis, macropinocytosis, and clathrin-mediated endocytosis typically fuse with lysosomes for degradation. And enzymes in lysosomes may also inhibit drug components and reduce therapeutic efficacy. In contrast, caveolae formed *via* caveolin-mediated endocytosis can partially evade lysosomal fusion and transport their contents to non-enzymatic compartments such as the smooth endoplasmic reticulum and the Golgi trans network, thereby protecting them from lysosomal degradation [160,161]. Research on the post-endocytic transport of tFNAs remains limited. In 2014, Fan's team used Cy3-labeled tFNAs to demonstrate significant co-localization with lysosomes within 12 h [154], a finding corroborated by subsequent studies indicating that tFNA uptake is mediated by macropinocytosis in HeLa cells [156]. Tang *et al.* ob-

served strong co-localization of FAM-labeled tFNAs with the endoplasmic reticulum, noting greater co-localization in 4T1 cells compared to BF cells [162]. Liu *et al*. reported co-localization of mitochondria with quantum dots after 6 h of incubation in HeLa cells, though co-localization signals were relatively weak. Similarly, co-localization between tFNAs and mitochondria has been observed in both human and mouse breast cancer cells [163,164]. Given the established endocytic mechanisms and potential delivery compartments of tFNAs, Cai *et al*. conducted a time-series experiment using Cy5-labeled tFNAs in human keratinocytes to investigate the co-localization dynamics with lysosomes, the endoplasmic reticulum, and mitochondria (Fig. S8 in Supporting information) [31]. Prolonged incubation revealed sequential co-localization of tFNAs with these organelles. Furthermore, the use of small molecule inhibitors confirmed that clathrin-mediated endocytosis of tFNAs was mainly directed into lysosomes, whereas caveolin-mediated endocytosis of tFNAs facilitates lysosomal escape and enables subsequent delivery to the endoplasmic reticulum and mitochondria (Fig. S9A in Supporting information). Despite these advances, research on the intracellular transport and localization of tFNAs remains insufficient and highly cell type-dependent. Current investigations rely primarily on fluorescence labeling-assisted confocal detection. To fully understand the intracellular transport processes of tFNAs, additional techniques such as transmission electron microscopy are needed. Elucidating these transport mechanisms will facilitate the development of subcellular structure-targeted drug delivery systems based on tFNAs and provide new insights into the fundamental mechanisms of tFNA action.

4.4. Subcellular targeting strategies

A comprehensive understanding of the transmembrane transport mechanisms and subcellular localization characteristics of tFNAs enables the rational design of smart drugs with subcellular targeting capabilities. Subcellular-targeted therapy represents a current research focus as it offers superior therapeutic advantages over conventional approaches by precisely directing therapeutic agents to specific organelles (*e.g.*, mitochondria, nuclei, and lysosomes) [165,166]. This approach significantly enhances drug concentration at target sites through ligand-guided accumulation in pathological organelles, enabling direct interventions in core disease mechanisms such as mitochondrial function restoration and gene expression modulation [167]. The stimuli-responsive design facilitates controlled drug release in response to organelle-specific microenvironmental cues, thereby improving therapeutic specificity while minimizing off-target effects [168]. Furthermore, subcellular precision delivery reduces systemic toxicity to healthy organelles and allows for real-time treatment monitoring by integrating diagnostic probes [169]. Such strategies not only expand the therapeutic window but also enable multidimensional interventions for complex diseases, driving a paradigm shift in precision medicine from tissue-level to subcellular-scale applications. tFNAs have been explored as versatile drug carriers at the subcellular level to maximize therapeutic efficacy [170]. Initial studies have shown that the early and rapid internalization of tFNAs is closely linked to the lysosomal pathway, which offers inherent advantages for passive lysosomal targeting. Inspired by the efficient uptake of tFNAs by macrophages *via* the lysosomal pathway, Cai's team developed a dynamic lysosome-activated tFNA-based nanobox to completely encapsulate short interfering RNA (siRNA) [32]. This nanobox undergoes conformational changes in response to the acidic lysosomal microenvironment, triggering siRNA release. Similarly, Fan's team used tFNAs to encapsulate zinc-responsive fluorophores, which were internalized *via* the lysosomal pathway to monitor zinc ion concentrations in living cells (Fig. S9B in Supporting information) [171]. Chen *et al*. modified the four vertices of tFNAs with Pr-Cl, Pr-Ca, Pr-pH, and Cy5, respectively [172]. Cy5 served as a stable reference signal, allowing for simultaneous *in situ* detection of Cl^-, Ca^{2+}, and pH within lysosomes and facilitating the identification of lysosome subpopulations with distinct characteristics. Mitochondrial targeting using tFNAs functionalized with triphenylphosphine (TPP) has also been extensively studied (Fig. S9C in Supporting information). Chen *et al*. utilized TPP-modified tFNAs to deliver a purine/apyrimidinic endonuclease 1 (APE1)-responsive molecular beacon, enabling the monitoring of APE1 levels in tumor cells to assess radiosensitivity [164]. Yang *et al*. employed this approach to dynamically construct G-quadruplexes using intracellular potassium ions, achieving controllable intracellular signal-driven assembly of tFNAs and mitochondrial function intervention [34]. This created a polyanion barrier outside the mitochondria, blocking inter-organelle communication and limiting energy supply to tumor cells. Tang *et al*. modified tFNAs with methyl sulfonamide groups to deliver glucose oxidase specifically to the endoplasmic reticulum, where the glucose consumption triggered the production of reactive oxygen species, inducing endoplasmic reticulum stress and enhancing cancer immunotherapy (Fig. S9D in Supporting information) [162]. Additionally, Shao's team [173] applied tFNAs at a more microscopic level. They developed a three-dimensional barcode system based on the tFNAs structure, termed STAMP, to measure the expression and subcellular distribution of various markers, including proteins, RNA, and metabolites. This method can theoretically provide over 10^9 barcodes, meeting the requirements for high-throughput and high-sensitivity analysis of protein expression and spatial distribution. Collectively, these advances highlight the significant potential of subcellular-targeted tFNA-based therapeutics in enhancing drug efficacy, reducing side effects, and enabling personalized treatment, offering new avenues for research on tFNA applications.

5. Challenges and optimization directions

tFNAs exhibit significant potential for clinical applications. However, there are still some key challenges must be addressed: (1) *In vivo* stability: While tFNAs demonstrate higher structural stability than single-stranded DNA, their rapid degradation in physiological environments remains a critical barrier [146]. Enhancing stability through chemical modifications, biomimetic encapsulation, and dynamic structural reinforcement is essential to prolonging circulation time. (2) Long-term biosafety: Although short-term biocompatibility has been confirmed [17,174], systematic evaluations of immunogenicity, metabolite toxicity, and organ accumulation under prolonged exposure are required. Additional assessments of engineered modifications are imperative to ensure human applicability. (3) Metabolic profiling: At present, there is a certain understanding of the *in vivo* biological distribution, cell entry pathways and intracellular transport of tFNAs, but more detailed research on metabolic mechanism needs to implemented. (4) Standard synthesis process: The programmability of tFNAs has led to extensive research work in engineering modifications [175]. But the absence of unified standards for reaction parameters, coupling efficiency, and quality control across different modification strategies hinders the broader application of tFNAs in the field of biomedicine and beyond. At present, there are some published synthesis protocols [18,176–178], yet other types of related schemes need to be further summarized and improved. (5) Scalability challenges: The current scalability challenges of tFNAs involve multiple dimensions, including product synthesis process, stability control, quality control, and cost-effectiveness. Scaling laboratory-based annealing methods to cost-effective industrial production is critical for commercialization of tFNAs. Optimization of these directions will play a key role in promoting the clinical application of tFNAs.

6. Conclusions and prospects

tFNA-based drug delivery systems have garnered increasing attention in biomedical research due to their unique advantages and potential. This review highlights recent advancements in the application of tFNAs as delivery carriers for organ and cell targeting. It discusses key aspects such as the various administration routes and their benefits, *in vivo* metabolism, intracellular transport mechanisms, and organelle-targeted interventions. Currently, subcellular-targeted drug delivery is advancing rapidly, with nanoscale carriers playing a pivotal role in developing advanced pharmaceutical formulations. These carriers exhibit excellent biocompatibility, the ability to deliver multiple drugs or act at multiple levels, modifiability, and passive biological targeting. By leveraging appropriate structural modifications or surface engineering, nanocarriers can be designed to achieve active targeting, enabling specific accumulation in certain tissues or subcellular structures. This targeted approach offers significant advantages in reducing toxicity and enhancing therapeutic efficacy. The unique nanoscale properties and programmability of tFNAs allow them to overcome the limitations of traditional delivery systems. They facilitate endosomal escape *via* energy-dependent endocytosis pathways and precisely target key organelles such as mitochondria, the endoplasmic reticulum, and lysosomes. These properties position tFNAs as promising candidates for subcellular-targeted delivery, broadening their applications in precision medicine, including gene editing and epigenetic regulation. However, the current understanding of tFNA internalization mechanisms and intracellular transport processes across different cell types remains limited. Research on the fundamental mechanisms underlying their tissue penetration abilities, such as transdermal mechanisms and axonal transport, is scarce, and the metabolic outcomes of tFNAs at the cellular and individual levels require further exploration. Future studies should integrate advanced biochemical technologies, such as multi-omics, to systematically elucidate the transmembrane transport regulations and metabolic pathways of tFNAs in complex biological environments. Particular attention should be paid to cell type-specific internalization mechanisms and their correlation with subcellular localization. Through specific engineering modifications, tFNAs can be optimized to achieve precise targeting and stable metabolism at the subcellular level. These comprehensive studies are expected to accelerate the clinical translation of tFNA-based therapeutics and provide a new generation of delivery platforms for the precision treatment of major diseases.

Declaration of competing interest

The authors declare that they have no known competing financial interests or personal relationships that could have appeared to influence the work reported in this paper.

CRediT authorship contribution statement

Wen Chen: Formal analysis, Data curation, Conceptualization. **Hao Wang:** Data curation. **Qiang Sun:** Formal analysis. **Shaojingya Gao:** Formal analysis. **Yunfeng Lin:** Conceptualization. **Yun Wang:** Data curation, Conceptualization. **Xiaoxiao Cai:** Writing – review & editing, Funding acquisition, Conceptualization.

Acknowledgments

This study was supported by National Natural Science Foundation of China (Nos. 82322015, 82171006) and Sichuan Province Youth Science and Technology Innovation Team (No. 2022JDTD0021), Sichuan Science and Technology Program (No. 2022NSFSC0002), West China Hospital of Stomatology Sichuan University (No. RCDWJS2024-3), Postdoctoral Fellowship Program of CPSF (No. GZC20231790).

Supplementary materials

Supplementary material associated with this article can be found, in the online version, at doi:10.1016/j.cclet.2025.111396.

References

[1] N.C. Seeman, J. Theor. Biol. 99 (1982) 237–247.
[2] S. Jiang, Z. Ge, S. Mou, et al., Chem 7 (2021) 1156–1179.
[3] H. Wang, Q. Liu, X. Lan, et al., Angew. Chem. Int. Ed. 61 (2022) e202111980.
[4] Q. Liu, Z. Ge, X. Mao, et al., Angew. Chem. 130 (2018) 7249–7253.
[5] Y. Zhang, X. Xie, W. Ma, et al., Nano Micro Lett. 12 (2020) 74.
[6] P.W.K. Rothemund, Nature 440 (2006) 297–302.
[7] N.C. Seeman, H.F. Sleiman, Nat. Rev. Mater. 3 (2018) 17068.
[8] K.E. Bujold, A. Lacroix, H.F. Sleiman, Chem 4 (2018) 495–521.
[9] L. Li, S. Nie, T. Du, et al., Med. Comm. Biomater. Appl. 2 (2023) e37.
[10] M. Lin, J. Wang, G. Zhou, et al., Angew. Chem. Int. Ed. 54 (2015) 2151–2155.
[11] M. Li, F. Yin, L. Song, et al., Chem. Rev. 121 (2021) 10469–10558.
[12] S. Zhao, R. Tian, J. Wu, et al., Nat. Commun. 12 (2021) 358.
[13] F. Yin, H. Zhao, S. Lu, et al., Nat. Nanotechnol. 18 (2023) 677–686.
[14] X. Wang, X. Zhao, Med. Comm. Biomater. Appl. 1 (2022) e17.
[15] R.P. Goodman, R.M. Berry, A.J. Turberfield, Chem. Commun. (2004) 1372–1373.
[16] Y. He, T. Ye, M. Su, et al., Nature 452 (2008) 198–201.
[17] S. Li, T. Tian, T. Zhang, et al., Mater. Today 24 (2019) 57–68.
[18] S. Li, T. Tian, T. Zhang, et al., Nat. Protoc. 20 (2024) 336–362.
[19] W. Wang, M. Lin, W. Wang, et al., Bioact. Mater. 33 (2024) 279–310.
[20] M. Zhou, Y. Lu, Y. Tang, et al., Biomaterials 318 (2025) 123183.
[21] Y. Yang, J. Yang, J. Zhu, et al., Bioact. Mater. 39 (2024) 191–205.
[22] J. Li, H. Pei, B. Zhu, et al., ACS Nano 5 (2011) 8783–8789.
[23] Q.S. Li, D. Zhao, X.R. Shao, et al., ACS Appl. Mater. Interfaces 9 (2017) 36695–36701.
[24] D.X. Xiao, Y.J. Li, T.R. Tian, et al., ACS Appl. Mater. Interfaces 13 (2021) 6109–6118.
[25] M. Zhang, X.L. Zhang, T.R. Tian, et al., Bioact. Mater. 8 (2022) 368–380.
[26] S.R. Shi, C. Yang, T.R. Tian, et al., Bone Res. 8 (2020) 6.
[27] R. Yan, W. Cui, W. Ma, et al., ACS Nano 17 (2023) 8767–8781.
[28] X. Chen, Z. Xu, Y. Gao, et al., Adv. Mater. 36 (2024) 2406118.
[29] T. Zhang, D. Xiao, M. Zhou, et al., Chin. Chem. Lett. 36 (2025) 110594.
[30] L. Bai, M. Feng, Q. Zhang, et al., Adv. Funct. Mater. 34 (2024) 2314789.
[31] Y.C. Ge, Q.X. Wang, Y.X. Yao, et al., Adv. Sci. 11 (2024) 2308701.
[32] Y. Gao, X. Chen, T. Tian, et al., Adv. Mater. 34 (2022) e2201731.
[33] S. Li, Y. Liu, T. Zhang, et al., Adv. Mater. 34 (2022) 2204287.
[34] F. Li, Y. Liu, Y. Dong, et al., J. Am. Chem. Soc. 144 (2022) 4667–4677.
[35] M. Zhang, Y. Wen, Z. Huang, et al., Chem. Eng. J. 454 (2023) 140399.
[36] J. Gu, J. Liang, T. Tian, et al., JACS Au 5 (2025) 486–520.
[37] Z. Ge, H. Gu, Q. Li, et al., J. Am. Chem. Soc. 140 (2018) 17808–17819.
[38] R. Veneziano, S. Ratanalert, K. Zhang, et al., Science 352 (2016) 1534 -1534.
[39] Z. Yang, L. Shi, Y. Wang, et al., Small 21 (2025) 2410162.
[40] R.P. Goodman, I.A. Schaap, C.F. Tardin, et al., Science 310 (2005) 1661–1665.
[41] J.-W. Keum, H. Bermudez, Chem. Commun. (2009) 7036–7038.
[42] A.S. Walsh, H. Yin, C.M. Erben, et al., ACS Nano 5 (2011) 5427–5432.
[43] T. Zhang, W. Cui, T. Tian, et al., ACS Appl. Mater. Interfaces 12 (2020) 47115–47126.
[44] S. Mazumdar, D. Chitkara, A. Mittal, Acta Pharm. Sin. B 11 (2021) 903–924.
[45] P. Makvandi, M. Chen, R. Sartorius, et al., Nano Today 40 (2021) 101279.
[46] J.J. Rennick, A.P.R. Johnston, R.G. Parton, Nat. Nanotechnol. 16 (2021) 266–276.
[47] F. Ding, S. Zhang, S. Liu, et al., Adv. Sci. 9 (2022) 2105947.
[48] T. Tian, C. Zhao, S. Li, et al., ACS Appl. Mater. Interfaces 15 (2023) 10492–10505.
[49] Y. Wen, M. Zhang, Y. Yao, et al., Chin. Chem. Lett. 34 (2023) 107549.
[50] S. Xu, X. Qin, J. Liang, et al., Cell Prolif. 57 (2024) e13637.
[51] M. Zhang, X. Qin, Y. Gao, et al., Adv. Sci. 10 (2023) 2303706.
[52] L. Yao, G. Zhang, Y. Wang, et al., Adv. Mater. 37 (2025) 2414336.
[53] G. Zhang, Y. Gao, L. Yao, et al., Adv. Funct. Mater. 35 (2025) 2419914.
[54] Y. Wu, J. Zhang, W. He, et al., Nano Biomed. Eng. 15 (2023) 199–224.
[55] M. Friedrich-Rust, T. Poynard, L. Castera, Nat. Rev. Gastroenterol. Hepatol. 13 (2016) 402–411.
[56] N.L. Gluchowski, M. Becuwe, T.C. Walther, et al., Nat. Rev. Gastroenterol. Hepatol. 14 (2017) 343–355.
[57] K.M. Tsoi, S.A. Macparland, X.Z. Ma, et al., Nat. Mater. 15 (2016) 1212–1221.
[58] J. Li, C. Chen, T. Xia, Adv. Mater. 34 (2022) 2106456.
[59] M. Cao, R. Cai, L. Zhao, et al., Nat. Nanotechnol. 16 (2021) 708–716.
[60] J. Li, X. Wang, K.-C. Mei, et al., Nano Today 37 (2021) 101061.
[61] Y. Chen, S. Shi, B. Li, et al., ACS Appl. Mater. Interfaces 14 (2022) 13136–13146.
[62] D. Zhang, L. Fu, Y. Yang, et al., Mater. Today Nano 25 (2024) 100454.
[63] M. Yu, J. Zheng, ACS Nano 9 (2015) 6655–6674.
[64] Z. Chen, H. Meng, G. Xing, et al., Toxicol. Lett. 163 (2006) 109–120.
[65] Y. Huang, X. Ning, S. Ahrari, et al., Nat. Rev. Nephrol. 20 (2024) 354–370.
[66] Q. Zhang, S. Lin, L. Wang, et al., Chem. Eng. J. 413 (2021) 127426.
[67] D.M. Teleanu, C. Chircov, A.M. Grumezescu, et al., Pharmaceutics 10 (2018) 269.

[68] N.J. Abbott, A.A. Patabendige, D.E. Dolman, et al., Neurobiol. Dis. 37 (2010) 13–25.
[69] X. Yang, F. Zhang, Y. Du, et al., Chin. Chem. Lett. 33 (2022) 1901–1906.
[70] W. Cui, Z. Guo, X. Chen, et al., Sci. Bull. 69 (2024) 3925–3935.
[71] Q. Wang, J. Cheng, F. Liu, et al., Adv. Sci. 11 (2024) 2306622.
[72] J. Zhu, Y. Yang, W. Ma, et al., Nano Lett. 22 (2022) 2381–2390.
[73] Y. Yang, J. Zhu, W. Ma, et al., Appl. Mater. Today 24 (2021) 101098.
[74] L. Tan, J. Xie, C. Liao, et al., J. Nanobiotechnol. 22 (2024) 682.
[75] V. Forest, J. Pourchez, Adv. Drug Deliv. Rev. 183 (2022) 114173.
[76] W. Zhong, X. Zhang, Y. Zeng, et al., Nano Res. 14 (2021) 2067–2089.
[77] X. Chen, J. He, Y. Xie, et al., Cell Prolif. 56 (2023) e13424.
[78] P. Pallagi, P. Hegyi, Z. Rakonczay, Pancreas 44 (2015) 1211–1233.
[79] C. Viegas, A.B. Patrício, J. Prata, et al., Pharmaceutics 15 (2023) 2363.
[80] Q. Zhang, S. Li, Y. Yu, et al., Int. J. Nanomed. 17 (2022) 4367.
[81] Y. Wang, Y. Li, S. Gao, et al., Nano Lett. 22 (2022) 1759–1768.
[82] S. Gao, M. Zhou, Y. Li, et al., ACS Appl. Mater. Interfaces 13 (2021) 50802–50811.
[83] G. Proctor, A. Shaalan, J. Dent. Res. 100 (2021) 1201–1209.
[84] X. Xie, W. Ma, G. Li, et al., Cell Prolif. 56 (2023) e13381.
[85] S. Gao, Y. Wang, Y. Li, et al., ACS Appl. Mater. Interfaces 13 (2021) 42543–42553.
[86] Y. Ding, Z. Li, A. Jaklenec, et al., Adv. Drug Deliv. Rev. 179 (2021) 113914.
[87] D.A. Blair, D.L. Turner, T.O. Bose, et al., J. Immunol. 187 (2011) 2310–2321.
[88] F. Shen, Z. Xiong, Y. Wu, et al., Angew. Chem. 135 (2023) e202301147.
[89] X. Qin, B. Zhang, X. Sun, et al., ACS Appl. Mater. Interfaces 15 (2023) 7793–7803.
[90] Y. Jiang, S. Li, T. Zhang, et al., ACS Appl. Mater. Interfaces 14 (2022) 15069–15079.
[91] L. Liu, W. Zhao, Q. Ma, et al., Nanoscale Adv. 5 (2023) 1527–1558.
[92] C. Wiraja, Y. Zhu, D.C.S. Lio, et al., Nat. Commun. 10 (2019) 1147.
[93] X. Lyu, H. Wu, M. Xu, et al., ACS Appl. Mater. Interfaces 16 (2024) 33192–33204.
[94] C. Qi, Q. Sun, D. Xiao, et al., Int. J. Oral Sci. 16 (2024) 30.
[95] Y. Xie, J. He, S. Li, et al., Adv. Funct. Mater. 33 (2023) 2303580.
[96] A.C. Bisen, A. Biswas, A. Dubey, et al., MedComm Biomater. Appl. 3 (2024) e77.
[97] Y.S. Kumar, C. Gurudeva, G. Sridevi, et al., Nano Biomed. Eng. 16 (2024) 510–519.
[98] A.L. Onugwu, C.S. Nwagwu, O.S. Onugwu, et al., J. Control. Release 354 (2023) 465–488.
[99] R. Herrero-Vanrell, M.V. De La Torre, V. Andrés-Guerrero, et al., J. Drug Deliv. Sci. Technol. 23 (2013) 75–102.
[100] N. Liu, X. Zhang, N. Li, et al., Small 15 (2019) 1901907.
[101] M. Loescher, C. Seiz, J. Hurst, et al., Pharmaceutics 14 (2022) 134.
[102] R. Wang, Y. Liu, W. Xiao, et al., ACS Appl. Mater. Interfaces 15 (2022) 541–551.
[103] F. Deschaseaux, L. Sensébé, D. Heymann, Trends Mol. Med. 15 (2009) 417–429.
[104] F. Peng, X. Zhang, Y. Wang, et al., Collagen Leather 5 (2023) 36.
[105] X. Luo, L. Ji, F. Ao, et al., Collagen Leather 6 (2024) 18.
[106] J. He, K. Li, T. Wu, et al., Med. Comm. Biomater. Appl. 2 (2023) e60.
[107] L.-N. Liu, P. Hu, Y. Liu, et al., ACS Appl. Mater. Interfaces 15 (2023) 25403–25416.
[108] Y. Li, J. Li, Y. Chang, et al., Chin. Chem. Lett. 35 (2024) 109414.
[109] T. Chen, D. Xiao, Y. Li, et al., Chin. Chem. Lett. 33 (2022) 2517–2521.
[110] R. Shi, Y. Zhu, W. Lu, et al., Chin. Chem. Lett. 36 (2024) 110241.
[111] Y. Li, Z. Cai, W. Ma, et al., Bone Res. 12 (2024) 14.
[112] A.E. Almada, A.J. Wagers, Nat. Rev. Mol. Cell Biol. 17 (2016) 267–279.
[113] Y. Gao, T. Zhang, J. Zhu, et al., Mater. Chem. Front. 4 (2020) 2731–2743.
[114] X. Yu, Y. Wang, L. Ran, et al., Nano Lett. 23 (2023) 8816–8826.
[115] A.F. Radu, S.G. Bungau, Cells 10 (2021) 2857.
[116] J. Lieberthal, N. Sambamurthy, C.R. Scanzello, Osteoarthr. Cartil. 23 (2015) 1825–1834.
[117] J. Pradal, P. Maudens, C. Gabay, et al., Int. J. Pharm. 498 (2016) 119–129.
[118] S. Liao, Z. Liu, W. Lv, et al., ACS Appl. Mater. Interfaces 16 (2024) 53499–53514.
[119] L. Fu, P. Li, J. Zhu, et al., Bioact. Mater. 9 (2022) 411–427.
[120] Y. Lin, Q. Li, L. Wang, et al., Int. J. Oral Sci. 14 (2022) 51.
[121] X. Zuo, Y. Xiao, J. Yang, et al., Collagen Leather 6 (2024) 33.
[122] D. Zhang, R. He, Y. Qu, et al., Med. Comm. Biomater. Appl. 3 (2024) e103.
[123] S. Lin, Q. Zhang, S. Li, et al., ACS Appl. Mater. Interfaces 12 (2020) 11397–11408.
[124] Y. Ge, Q. Wang, X. Qin, et al., ACS Appl. Mater. Interfaces 14 (2022) 19091–19103.
[125] B. Tang, Y. Yang, Y. Li, et al., Chem. Eng. J. 495 (2024) 153249.
[126] J. Scheib, A. Höke, Nat. Rev. Neurol. 9 (2013) 668–676.
[127] Y. Yao, Y. Wen, Y. Li, et al., Nanoscale 13 (2021) 15598–15610.
[128] J. Li, Y. Yao, Y. Wang, et al., Adv. Mater. 34 (2022) 2202513.
[129] L. Wang, Q. Yao, X. Guo, et al., J. Nanobiotechnol. 22 (2024) 392.
[130] L.R. Orrick, M.O.J. Olson, H. Busch, Proc. Natl. Acad. Sci. U. S. A. 70 (1973) 1316–1320.
[131] N.A. Fonseca, A.S. Rodrigues, P. Rodrigues-Santos, et al., Biomaterials 69 (2015) 76–88.
[132] M. Alibolandi, M. Ramezani, K. Abnous, et al., J. Pharm. Sci. 105 (2016) 1741–1750.
[133] D. Xiao, T. Chen, T. Zhang, et al., Chin. Chem. Lett. 35 (2024) 108602.
[134] S. Li, T. Zeng, Z. Wu, et al., J. Am. Chem. Soc. 147 (2025) 2168–2181.
[135] W. Guo, H. Gao, H. Li, et al., ACS Appl. Mater. Interfaces 14 (2022) 31634–31644.
[136] M. Kumar, U. Kumar, A.K. Singh, Nano Biomed. Eng. 14 (2022) 38–52.
[137] Z. Xia, P. Wang, X. Liu, et al., Biochemistry 55 (2016) 1326–1331.
[138] C. Zhang, M. Han, F. Zhang, et al., Int. J. Nanomed. 15 (2020) 885–900.
[139] W. Ma, Y. Yang, J. Zhu, et al., Adv. Mater. 34 (2022) 2109609.
[140] T. Tian, J. Li, C. Xie, et al., ACS Appl. Mater. Interfaces 10 (2018) 3414–3420.
[141] S.D. Perrault, W.M. Shih, ACS Nano 8 (2014) 5132–5140.
[142] Y. Yang, J. Wang, H. Shigematsu, et al., Nat. Chem. 8 (2016) 476–483.
[143] R.R. Du, E. Cedrone, A. Romanov, et al., ACS Nano 16 (2022) 20340–20352.
[144] W. Yin, X. Chen, L. Bai, et al., Biomaterials 319 (2025) 123194.
[145] N. Song, H. Li, C. Yao, et al., Acc. Chem. Res. 57 (2024) 2763–2774.
[146] Y. Guo, Y. Huang, M. Liu, et al., Small Methods 9 (2025) 2401007.
[147] X. Chao, Y. Yang, W. Gong, et al., J. Cell Biol. 223 (2024) e202401110.
[148] H.T. Mcmahon, E. Boucrot, Nat. Rev. Mol. Cell Biol. 12 (2011) 517–533.
[149] A. Banerjee, A. Berezhkovskii, R. Nossal, Phys. Biol. 13 (2016) 016005.
[150] L. Pelkmans, A. Helenius, Traffic 3 (2002) 311–320.
[151] D. Manzanares, V. Ceña, Pharmaceutics 12 (2020) 371.
[152] D. Lingwood, K. Simons, Science 327 (2010) 46–50.
[153] A. Rajwar, S.R. Shetty, P. Vaswani, et al., ACS Nano 16 (2022) 10496–10508.
[154] L. Liang, J. Li, Q. Li, et al., Angew. Chem. Int. Ed. 53 (2014) 7745–7750.
[155] H. Ding, J. Li, N. Chen, et al., ACS Cent. Sci. 4 (2018) 1344–1351.
[156] T. Tian, C. Zhang, J. Li, et al., Small 17 (2021) 2100837.
[157] T. Zhang, M. Zhou, D. Xiao, et al., Adv. Sci. 9 (2022) 2202058.
[158] Y. Ge, T. Tian, X. Shao, et al., ACS Appl. Mater. Interfaces 11 (2019) 27588–27597.
[159] S.P. Narayan, C.H.J. Choi, L. Hao, et al., Small 11 (2015) 4173–4182.
[160] S. Patel, J. Kim, M. Herrera, et al., Adv. Drug Deliv. Rev. 144 (2019) 90–111.
[161] Y. Song, Y. Wu, L. Xu, et al., ACS Nano 15 (2021) 8267–8282.
[162] Y. Li, X. Zhang, X. Wan, et al., Adv. Funct. Mater. 30 (2020) 2000532.
[163] Y. Liu, Y.-J. Wang, Y. Du, et al., Proc. Natl. Acad. Sci. U. S. A. 121 (2024) e2317492121.
[164] J. Yan, J. Chen, N. Zhang, et al., J. Mater. Chem. B 8 (2020) 492–503.
[165] Y. Cheng, Z. Qu, Q. Jiang, et al., Adv. Mater. 37 (2025) 2305095.
[166] Q. Qin, M. Wang, Y. Zou, et al., MedComm Biomater. Appl. 2 (2023) e65.
[167] F. Yu, X. Li, C. Sheng, et al., Angew. Chem. 136 (2024) e202409351.
[168] T. Sun, C. Jiang, Adv. Drug Deliv. Rev. 196 (2023) 114773.
[169] S.K. Pramanik, A. Das, Chem. Commun. 57 (2021) 12058–12073.
[170] L. Rajendran, H.J. Knoelker, K. Simons, Nat. Rev. Drug Discov. 9 (2010) 29–42.
[171] Y. Gao, X. Liu, W. Li, et al., Natl. Sci. Rev. 11 (2024) nwae307.
[172] G.Y. Zou, F. Bi, Y.L. Yu, et al., Anal. Chem. 96 (2024) 16639–16648.
[173] N.R. Sundah, N.R.Y. Ho, G.S. Lim, et al., Nat. Biomed. Eng. 3 (2019) 684–694.
[174] K. Xia, H. Kong, Y. Cui, et al., ACS Appl. Mater. Interfaces 10 (2018) 15442–15448.
[175] J. Li, R. Yan, S. Shi, et al., Expert Opin. Drug Deliv. 20 (2023) 1511–1530.
[176] T. Tian, T. Zhang, S. Shi, et al., Nat. Protoc. 18 (2023) 1028–1055.
[177] Y. Chen, M. Lin, D. Ye, et al., Nat. Protoc. 19 (2024) 985–1014.
[178] T. Zhang, T. Tian, R. Zhou, et al., Nat. Protoc. 15 (2020) 2728–2757.